



## **Investigation the Electrical Characteristics and the Sensing Behavior of Thin Cd<sub>2</sub>Si<sub>1-x</sub>Ge<sub>x</sub>O<sub>4</sub> Films**

Iqbal Sahham Naji

Assistant Professor, Physics Dept., Science College, University of Baghdad Baghdad / IRAQ

### **ARTICLE INFO**

#### **Article history:**

Received 12 March 2015

Accepted 28 June 2015

Available online 22 July 2015

#### **Keywords:**

Oxides, Thin Films, PLD method, Optical properties, Heterojunction, Gas sensors.

### **ABSTRACT**

Amorphous thin Films of Cd<sub>2</sub>Si<sub>1-x</sub>Ge<sub>x</sub>O<sub>4</sub> compound with different ratio of germanium (0, 0.3, 0.6) elements were prepared on glass and Si wafer substrate at room temperature by Pulsed- Laser Deposition (PLD). The optical band gap was found to be in the range (2.25-2.65 eV), when the Ge concentration changes from zero to 0.6. The sign of Hall coefficient was negative (n-type electrical conduction),with high mobility of order 10<sup>2</sup> cm<sup>2</sup>V<sup>-1</sup>s<sup>-1</sup>. The impact of Ge ratio on the electrical properties of Cd<sub>2</sub>Si<sub>1-x</sub>Ge<sub>x</sub>O<sub>4</sub> /Si heterostructure diodes was studied. The capacitance-voltage characteristic at frequency equals to 100 kHz gave an indicated that these diodes are abrupt type, and the capacitance increases while the width of depletion layer decreases with increase Ge concentration. The current-voltage measurements of these diodes shows that the mechanism of transport current coincide with recombination-tunneling model, where the ideality factor and rectification coefficient increase with increasing Ge ratio. The gas sensing results revealed that the Cd<sub>2</sub>Si<sub>0.7</sub>Ge<sub>0.3</sub>O<sub>4</sub> film has high sensitivity (73%) and fast rise time to NO<sub>2</sub> gas at room temperature compared with other compositions.

© 2015 AENSI Publisher All rights reserved.

To Cite This Article: Iqbal Sahham Naji., Investigation the Electrical Characteristics and the Sensing Behavior of Thin Cd<sub>2</sub>Si<sub>1-x</sub>Ge<sub>x</sub>O<sub>4</sub> Films. *Aust. J. Basic & Appl. Sci.*, 9(23): 551-560, 2015

## **INTRODUCTION**

Thin films technique is one of the most recent fully-fledged technologies that greatly contribute to developing the study of semiconductors by giving a clear indication of their chemical and physical properties (Alnaimi,S.M.,2007). Transparent electronics is emerging as one of the most promising technologies for future electronic products, as distinct from the traditional silicon technology (Barquinha, P.,2012) .Transparent conductive oxide films (TCOs), which are derivated from wide band-gap semiconductors with low specific resistance and high transparency in the visible wavelength range, have found wide applications in recent years as transparent electrodes in photovoltaics, flat panel displays, de-icers and electrochromic devices and their high reflectivity in the infrared (IR) makes them useful heat reflectors (Kumaravel, R., 2010). And electrochromics such as smart mirrors , solar cells, abrasion resistance coatings , corrosion resistant coatings, gas sensors, ohmic contacts to surface-emitting lasers, ohmic contacts to photodetectors, Shottky contacts to photodetectors, and heat mirrors for energy efficient windows and light bulbs (Abd El-Raheem, M.,2012).

Germanium is a chemical element with symbol Ge and atomic number 32. It is a lustrous,

hard, grayish-white metalloid in the carbon group, chemically similar to its group neighbors tin and silicon. Purified germanium is a semiconductor, with an appearance most similar to elemental silicon. Like silicon, germanium naturally reacts. Two oxides of germanium are known: germanium dioxide, (GeO<sub>2</sub>, germania) and germanium monoxide, (GeO). The dioxide, GeO<sub>2</sub> can be obtained by roasting germanium disulfide (GeS<sub>2</sub>), and is a white powder that is only slightly soluble in water but reacts with alkalis to form germinates (Masanori, K.,2002). The monoxide, germanous oxide, can be obtained by the high temperature reaction of GeO<sub>2</sub> with Ge metal (Washio, K., 2003). GeO<sub>2</sub> is a transparent conductive oxide (TCO) with a high potential in optoelectronics. Its band gap energy (5 eV), higher than other TCO materials, makes this oxide attractive as host for optical impurities to develop luminescent devices, from the ultraviolet-blue to the near-infrared range. GeO<sub>2</sub>, as other semiconductor oxides, has oxygen deficiency associated to its high concentration of oxygen vacancies, and this effect is more acute in nanowires due to the higher surface-volume ratio.

These defects are, in many cases, responsible for their smart optical and electrical properties and are the key factor in order to exploit them in practical devices, such as sensors or optoelectronic devices (Hidalgo, P.,2009).

**Corresponding Author:** Iqbal Sahham Naji, Assistant Professor, Physics Dept., Science College, University of Baghdad Baghdad / IRAQ

$\text{GeO}_2$  is a blue-green luminescent material with optical properties which are considered of interest for optoelectronic communications, so the fabrication of  $\text{GeO}_2$  nanowires would be useful to future optical nanodevices (Hidalgo,P.,2007). The dioxide (and the related oxides and germanates) exhibits the unusual property of having a high refractive index for visible light, but transparency to infrared light(Geological, S., 2008).

Germanium-based systems, such as germanosilicates, Si-Ge alloys, or  $\text{GeO}_2$  glasses, have been explored as hosts for RE ions in order to reach greater optoelectronic integration(Geological, S., 2008).

Silicon-germanium compounds are rapidly becoming an important semiconductor material, for use in high-speed integrated circuits. Circuits utilizing the properties of Si-SiGe junctions can be much faster than those using silicon alone. Silicon-germanium is beginning to replace gallium arsenide ( $\text{GaAs}$ ) in wireless communications devices (Geological, S., 2008). The SiGe chips, with high-speed properties, can be made with low-cost, well-established production techniques of the silicon chip industry (Teal, H.,1976).

Narushima,S., et al.,(2000) prepared amorphous  $2\text{CdO}.\text{GeO}_4$  by RF sputtering. They found that Fermi level of this amorphous material may be controlled by proton implantation, where the dc conductivity at 300K increased from  $10^{-9}$  to  $10 \text{ S.cm}^{-1}$  and its activation energy fell from 1eV to almost zero(degenerate state).

This article deals with the preparation of  $\text{Cd}_2\text{Si}_{1-x}\text{Ge}_x\text{O}_4$  thin films using pulsed laser deposition technique and reports the effect of chemical substitution of Ge for Si on the morphological , optical and electrical properties of these films and characterization the electrical properties of  $\text{Cd}_2\text{Si}_{1-x}\text{Ge}_x\text{O}_4/\text{Si}$  photodiodes, also evaluation the sensing properties of  $\text{Cd}_2\text{Si}_{1-x}\text{Ge}_x\text{O}_4$  gas sensors deposited on Si .

## MATERIALS AND METHODS

Samples of  $\text{Cd}_2\text{Si}_{1-x}\text{Ge}_x\text{O}_4$  were prepared by powder technology of mixtures of  $\text{SiO}_2$ ,  $\text{GeO}_2$  and  $\text{CdO}$  , the three oxides pre – calcined at 500 °C for 1 hour to remove hydroxide and carbonate impurities . After being weighted out in the appropriate molar ratios, ( $x = 0, 0.3, 0.6$ ), the powder were intimately mixed by hand grinding and reacted at 900 °C for 12 hour . Then pressed into a 13 mm diameter pellet at 4 Mpa and lightly sintered in air at 850 °C for 48 h.  $\text{Cd}_2\text{Si}_{1-x}\text{Ge}_x\text{O}_4$  thin films were prepared by Pulsed Laser Deposition (PLD) onto glass and Si wafers as substrates to study optical and electrical properties of the films and I-V and C-V characteristics of the heterojunctions, respectively. The deposition was carried out by using Nd-YAG laser with a wavelength of 1064 nm, Laser energy of

700mJ,repetition rate of 6 Hz, pulse duration of 10 ns, number of pulses equal to 400, and the vacuum is  $8*10^{-3}$  mbar. The distance between the base and the target is (1 cm). The crystallographic structure of prepared films were analyzed with diffractometer using Shimadzu 6000, with Cu-K $\alpha$  radiations operated at (40)KV and (30)mA , with scanning angle 20°-60° . The morphological surface analysis was investigated by using atomic force microscope (AA3000,Scanning probe microscope (SPM)). Double beam UV- Visible spectrophotometer was used to recorded the transmittance and absorbance spectra at room temperature in the wavelength range 200-1100 nm. In order to measure the electrical properties, ohmic contacts are needed. It was obtained by evaporated under vacuum of Al wire of high purity. The best condition for good ohmic contact was satisfied by a layer of 200 nm . Electrical properties were carried out by using Hall effect measurement system (3000 HMS ,VER 3.5, Ecopia).

Laser interferometer was used to measure the film thickness ,which was in the range (200± 20)nm.

The capacitance-voltage characteristics of the heterojunctions were measured using LRC apparatus type (Agileut 429 uA Precision Impedance Analyzet) at frequency 100 kHz .

Capacitance at different reverse bias voltage at the range (0-1) volt was measured to determine the type of the heterojunction (abrupt or graded), the value of built-in voltage ( $V_D$ ), and the width of the junction .

The current – voltage measurements for  $\text{Cd}_2\text{Si}_{1-x}\text{Ge}_x\text{O}_4/\text{Si}$  heterojunctions in the dark were studied by using Keithly Digital Electrometer 616 and D.C. power supply. The bias voltage varies between (0-2) volt for forward and reverse connection. I –V measurements under the illumination were made when they were exposed to Halogen Lamp type Philips 120 W at intensity (32) mW/cm<sup>2</sup> , using Keithly Digital Electrometer 616 , voltmeter , and D.C. power supply under forward and reverse bias voltage which was in the range (0-2) volt. The gas sensing properties were evaluated at room temperature by measuring the changes of resistance of the sensor in air and in the  $\text{NO}_2$  gas.

## RESULTS AND DISCUSSIONS

### a- Properties of Thin Films

X-ray diffraction (XRD) measurement provide insight into the structural properties of the  $\text{Cd}_2\text{Si}_{1-x}\text{Ge}_x\text{O}_4$  films. XRD patterns show all films have amorphous structure.

Fig. 1 shows the AFM micrographs of the  $\text{Cd}_2\text{Si}_{1-x}\text{Ge}_x\text{O}_4$  films with different x values (0,0.3 , 0.6). The two and three dimensional AFM images show continuous, uniform, and homogenous distribution film surface. The films have morphological characterization of eggs shape grains in big clusters varying in the range of average

diameter (89.77 -85.89nm), the surface features of the films are comparable and the calculated surface

roughness values change from 1.62 to 1.21 nm with increasing x value, as illustrate in Table 1.

**Table 1:** The grain size and roughness for thin  $\text{Cd}_2\text{Si}_{1-x}\text{Ge}_x\text{O}_4$  films

x	Average diameter(nm)	Roughness average (nm)	Root mean square (nm)
0	89.77	1.62	1.87
0.3	97.49	1.54	1.78
0.6	85.89	1.21	1.4

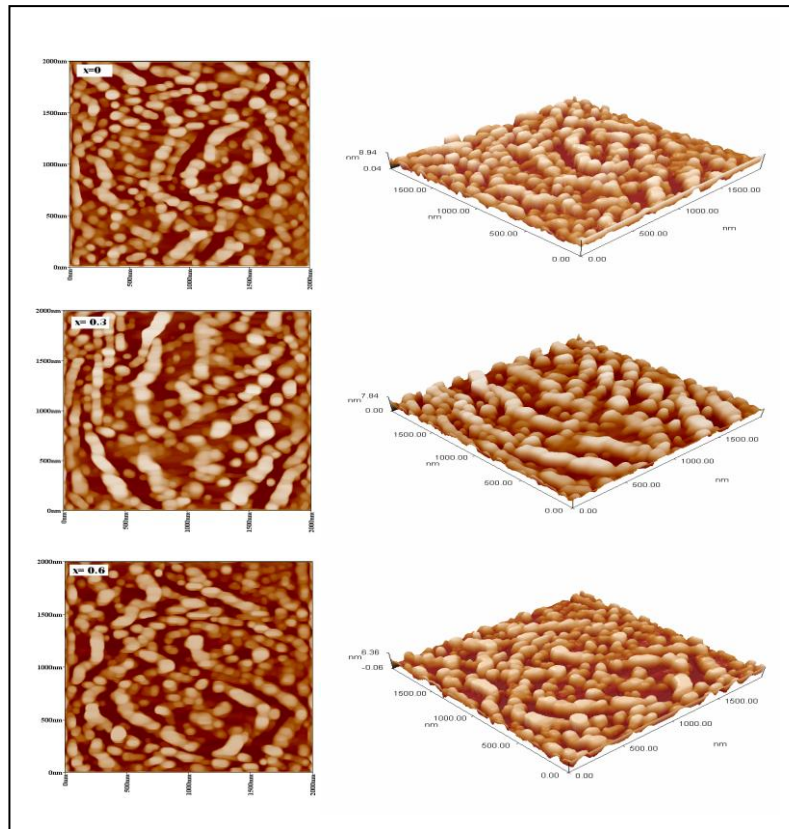


**Fig. 1:** Two and Three-D AFM images of thin  $\text{Cd}_2\text{Si}_{1-x}\text{Ge}_x\text{O}_4$  films at different x values.

UV-Visible and near-infrared transmission spectra of the  $\text{Cd}_2\text{Si}_{1-x}\text{Ge}_x\text{O}_4$  films of different x values (0, 0.3, 0.6) and of 200 nm thickness deposited on glass substrate have been recorded as shown in Fig.2. This figure shows the profoundly influence of Ge content on the optical properties of the films. All films have medium transmittance in the visible and NIR region (500-1100nm), which is change from 20 to 65% for x=0, and from 26 to 55% for x=0.3 and 0.6.

The effect of Ge concentration in the present work led to a shift of the fundamental optical absorption edge toward the UV from 550 to 468 nm due to an increase in the Ge concentration.

The direct band-gap is based on the extrapolated linear regression of the curve resulting from a plot of photon energy ( $h\nu$ ) versus  $(\alpha h\nu)^2$ . The absorption coefficient was calculated according to the equation[3]  $\alpha = (1/t) \ln (1/T)$ , where t is the thickness of the film and T is the transmittance at the wavelength.

The calculated direct band-gap value increased from 2.25 to 2.65 eV, when Ge increased from 0 to 0.6 respectively, as shown in Fig.3. This is mainly due the formation new band in gap, which causes a strong modification of the joint density of states and consequently the absorption spectrum (Ikhmayies, S., 2010).

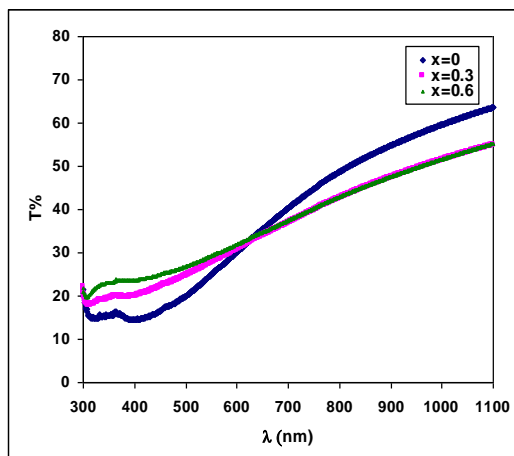


**Fig. 2:** Transmittance vs. wavelength at different x values.

This result coincides some way with the result of Salman, Gh.,(2014) who found the energy band of CdO films which prepared by PLD was 2.3 eV and the band gap of  $\text{Cd}_2\text{GeO}_4$  was 3.4 eV which found by Narushima, S., *et al.* (2000), this mean the energy gap increases with increasing Ge concentration in the film.

Fig.4 shows the variation in refractive index as a function of wavelength. It is worth noting that the refractive index of  $\text{Cd}_2\text{Si}_{1-x}\text{Ge}_x\text{O}_4$  films increase with

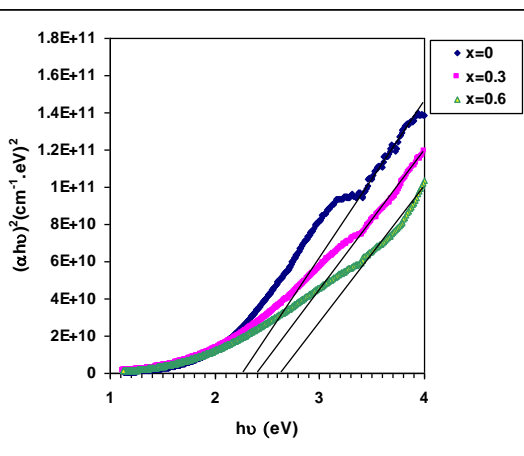


**Fig. 3:**  $(\alpha h\nu)^2$  vs.  $(h\nu)$  plots at different x values.

increasing x concentration. This increasing is associated with the reflection of the films.

The relation between the extinction coefficient and the wavelength of  $\text{Cd}_2\text{Si}_{1-x}\text{Ge}_x\text{O}_4$  films with different x value are shown in Fig.5 , where the extinction coefficient decrease with increase the x value. The rise and the fall in the extinction coefficient is directly dependent on the light absorption.

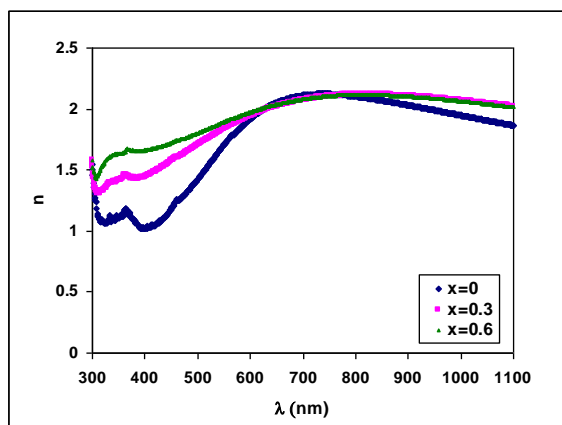


**Fig. 4:** The refractive index vs. the wavelength at different x values.

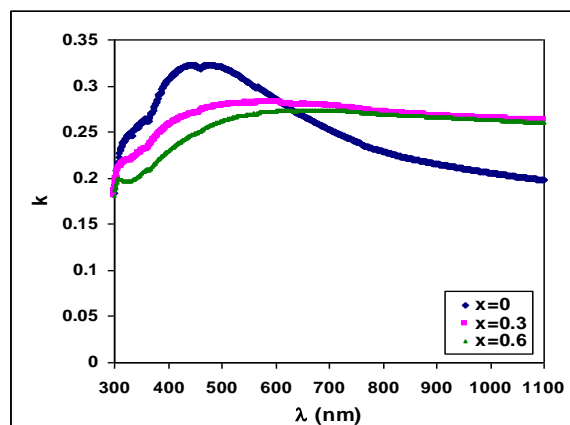


**Fig. 5:** The extinction coefficient vs. the wavelength at different x values.

The behavior of real part ( $\epsilon_r$ ) which represents the normal dielectric constant and imaginary part ( $\epsilon_i$ ) which represents the absorption associated with free carriers is the same as that of refractive index and extinction coefficient, respectively.

The optical properties parameters including, absorption coefficient , optical energy gap, and

optical constants (refractive index, extinction coefficient, real and imaginary part of the dielectric constant) at wavelength equals to 500 nm for thin  $Cd_2Si_{1-x}Ge_xO_4$  films have different values of x are listed in Table 2.

**Table 2:** The optical properties parameters of thin  $Cd_2Si_{1-x}Ge_xO_4$  films at different x values.

x	$\alpha \times 10^3 (cm^{-1})$	$E_g (eV)$	n	k	$\epsilon_r$	$\epsilon_i$
0	8.05	2.25	1.423	0.320	1.922	0.911
0.3	6.99	2.40	1.701	0.278	2.816	0.946
0.6	6.58	2.65	1.801	0.261	3.177	0.943

The electrical properties were estimated by Hall effect measurements for thin  $Cd_2Si_{1-x}Ge_xO_4$  films at different x values. This measurement shows a negative Hall coefficient, this means that the  $Cd_2Si_{1-x}Ge_xO_4$  films are n-type defect semiconductors, and the conductivity of these films is mainly attributed to oxygen deficiency which provides the donor states. This result coincides with the result of Narushima,S., *et al.* (2000)], who found that the sign of Hall and seebeck coefficients were negative for  $Cd_2GeO_4$  films.

The charge carrier concentration increases from  $2.05 \times 10^{16}$  to  $2.83 \times 10^{17} cm^{-3}$  when Ge concentration change from zero to 0.6, and this is obviously lead to increase the electrical conductivity of these films.

High charge mobility values were obtain for thin  $Cd_2Si_{1-x}Ge_xO_4$  films ,which is larger by several orders of magnitude than that of existing amorphous semiconductors. Table 3 summaries the values of electrical parameters of thin  $Cd_2Si_{1-x}Ge_xO_4$  films.

**Table 3:** The electrical properties parameters of thin  $Cd_2Si_{1-x}Ge_xO_4$  films at different x values.

x	type	$\sigma_{R.T} (\Omega.cm)^{-1}$	$n_H \times 10^{16} (cm^{-3})$	$\mu_H \times 10^2 (cm^2/V.s)$
0	n	0.743	2.05	2.20
0.3	n	17.08	22.10	3.32
0.6	n	19.22	28.30	4.24

#### b- Properties of $Cd_2Si_{1-x}Ge_xO_4/Si$ Heterojunctions:

The electrical properties, which include the I-V and C-V characteristic measurement of  $Cd_2Si_{1-x}Ge_xO_4/Si$  heterojunctions at different x values have been carried.

The junction capacitance variations as a function of reverse bias (0-1) volt of  $Cd_2Si_{1-x}Ge_xO_4 /Si$  heterojunction with different Ge concentration (0, 0.3, 0.6) at frequency equal to 100 kHz are shown in Fig.6 .

This measurement was achieved in order to get an idea about the impurity distribution in the vicinity of the junction, and to calculate the built in potential ( $V_D$ ).

It is worth noting that the capacitance decreases with increasing reverse bias, this behavior was due to an increase in the depletion region width, and this reduction was non-linear.

Additionally, it is clear that the capacitance at zero bias voltage ( $C_o$ ) increases from 0.57 to 2.84 nF when x change from zero to 0.6 .

This behavior was attributed to increases the carrier concentration when the Ge concentration increases in the  $Cd_2Si_{1-x}Ge_xO_4$  composition, which leads to increase the capacitance and as a result the depletion region width decreases, which means the reduction in Ge concentration lead to more diffusion for carrier of  $Cd_2Si_{1-x}Ge_xO_4$  films.

The width of the depletion region (W) has a high value when Ge concentration equal to zero. It is clear that the values of depletion region width was very low (narrow) , this is attributed to the low diffusion of these oxide films in Si wafer at room temperature (without substrate heating) which prepare by PLD technique.

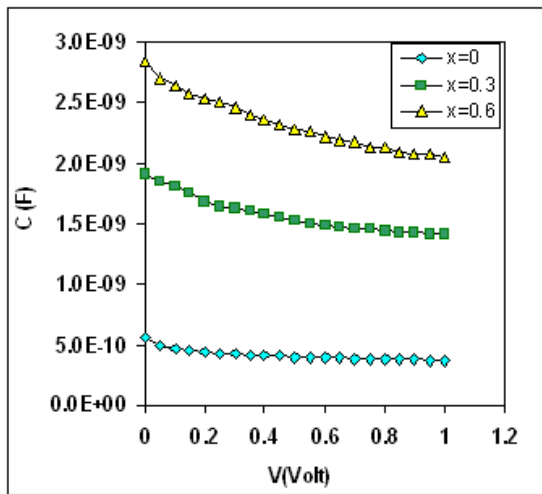


**Fig. 6:** The relation between capacitance and reverse applied voltage for  $\text{Cd}_2\text{Si}_{1-x}\text{Ge}_x\text{O}_4/\text{Si}$  diodes of different  $x$  values.

Fig. 7 reveals the variation of the inverse capacitance squared as a function of the reverse bias voltage. The linearity behavior of this plot confirms that the junction is abrupt type. It is observed from the figure that the built-in potential which represents the intersection ( $1/C^2$ ) of the straight line with the voltage axis, which increases with the increase of Ge ratio in the compound  $\text{Cd}_2\text{Si}_{1-x}\text{Ge}_x\text{O}_4$  systematically, and this is due to the enhancement of the distribution of Ge in the films (Amaechi, C. I., 2011).

The impurity concentration of donors can be calculated from the slope of the best fit straight line

of the same plots by using relation (Milnes, A.G., 1972)

$$\frac{1}{C^2} = \left[ \frac{2(\epsilon_1 N_{A1} + \epsilon_2 N_{D2})}{qN_{D2}N_{A1}} \right] (V_D - V_a) \quad (1)$$

Where  $[2(\epsilon_1 N_{A1} + \epsilon_2 N_{D2})/qN_{D2}N_{A1}]$  represent the slope,  $N_{A1}$  and  $N_{D2}$  are the accepter and donor concentrations, and  $\epsilon_1$ ,  $\epsilon_2$  are the dielectric constant of p-type and n-type semiconductor respectively.  $V_D$  is the built-in potential,  $V_a$  is the applied voltage.

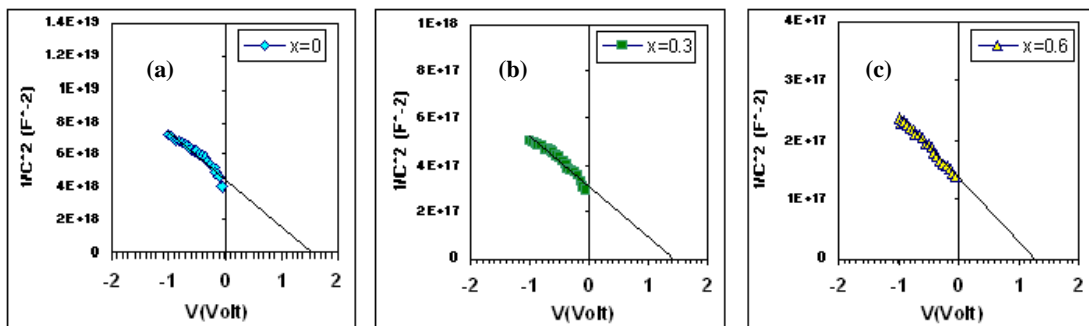


**Fig. 7:** The variation of  $1/C^2$  as a function of reverse bias voltage for  $\text{Cd}_2\text{Si}_{1-x}\text{Ge}_x\text{O}_4/\text{Si}$  diodes of different Ge values.

It can be observed that the carrier concentration increases with increasing the Ge concentration in the  $\text{Cd}_2\text{Si}_{1-x}\text{Ge}_x\text{O}_4$  films, and this behavior enhanced by Hall effect measurement.

All parameters which are calculated from this measurement are listed in Table 4

**Table 4:** The parameters which obtained from C-V characteristics for  $\text{Cd}_2\text{Si}_{1-x}\text{Ge}_x\text{O}_4/\text{Si}$  diodes with different  $x$  values.

$x$	$V_D$ (Volt)	$C_o$ (nF)	$W$ ( $\mu\text{m}$ )	$N_D \times 10^{16}$ ( $\text{cm}^{-3}$ )	$t_r$ (nsec)	$t_{\text{response}}$ (nsec)
0	1.55	0.57	0.111	1.306	28.5	12.95
0.3	1.40	1.91	0.034	4.532	95.5	43.40
0.6	1.23	2.84	0.023	4.940	142.0	64.54

Current-voltage characteristics is the more necessary analysis to specify the current transport mechanisms which determined the performance of the diode.

Fig. 8 shows the J-V characteristic of anisotype  $\text{Cd}_2\text{Si}_{1-x}\text{Ge}_x\text{O}_4$  /Si heterojunctions of different x concentrations at forward and reverse bias voltage in the dark within the range (0-2) volt.

The striking feature of these curves is non-ohmic behavior where it is very clear. Relatively freely current flows in the forward direction, but very low current flows in reverse direction, So the junctions have relatively good diode rectification characteristics at 2 volt. This means these junctions have high rectification coefficient (R.F), and it is increases considerably with increasing Ge

concentration in the  $\text{Cd}_2\text{Si}_{1-x}\text{Ge}_x\text{O}_4$  films as shown in Table 5.

In general the forward dark current is generated due to the flow of majority carriers and the forward applied voltage inject majority carriers, which lead to decrease the width of the depletion layer, and the value of built in potential reduce.

This J-V plot is consistent with Schockley equation (Sharma, B.L.,1974)

$$I = I_s [\exp(qV/\beta kT) - 1] \quad (2)$$

where  $I_s$  is the saturation current,  $q$  is the electron charge,  $k$  is the Boltzman constant,  $T$  is the absolute temperature, and  $\beta$  is the ideality factor which determines the dominant carrier transport mechanism.

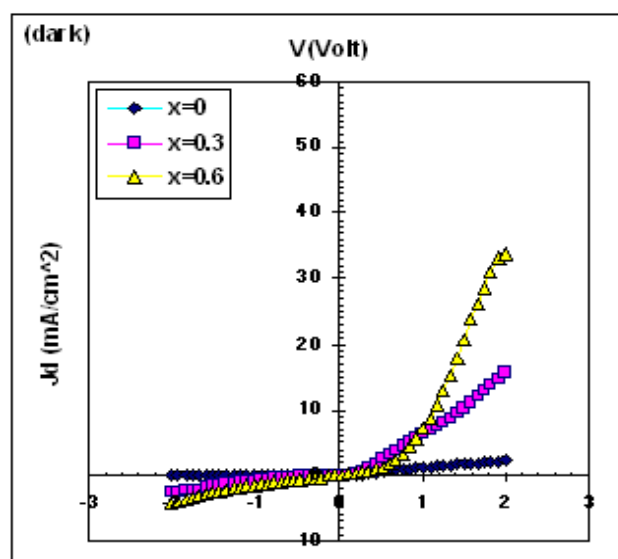


**Fig. 8:** J-V Characteristics for  $\text{Cd}_2\text{Si}_{1-x}\text{Ge}_x\text{O}_4$  /Si diodes at forward and reverse bias voltage of different x values.

This factor can be obtained from the slope of the linear dependence of  $\ln(I)$  on the forward bias voltage (Sarusi, G.,1994).

It is obvious that there are two region in the J-V plot, the first region represent forward bias region ,where the resistance determined by the series resistance ( $R_s$ ). In the second region (reverse bias region), the influence of shunt resistance ( $R_{sh}$ ) predominates (Wenus, J.,2003).

From the same figure, it is worth noting that the current increases with increasing Ge concentration, this may be due to increase the charge carrier concentration as the Ge concentration increases to 0.6 as emphasized by Hall effect measurements.

A semi-log I-V plot of the forward diode current as a function of applied voltage (0-0.4)volt is presented in Fig. 9 .There are two region can be distinguished ,the first in the range (0-0.2) volt, where the  $\beta$  can calculated from it. The value of ideality factor is ranged between (1.977-2.50), these values reflect that the carriers transport is taken place by tunneling and recombination mechanisms. From

the second region, the tunneling constant ( $A_t$ ) can be calculated by using the following equation

$$A_t = [d \ln (I_f/I_{S2})]/dV \quad (3)$$

The high values of ideality factor (greater than unity) generally is due to structural defects (Kim, W.,2002) and the interfacial oxide layer (Mousa, A. M., 2011).

Also the reverse bias current contains two regions. The first is the generation current, which depend on the bias voltage. The bias voltage increment leads to an increment in the depletion layer width, which in turn increases generation current. While the second which represent the stabilizes current region and becomes independent of the bias voltage, this is called the diffusion current (Ismail, R.A.,2003).

All parameters which calculated from J-V characteristics for  $\text{Cd}_2\text{Si}_{1-x}\text{Ge}_x\text{O}_4$  /Si diodes are illustrated in Table 5.

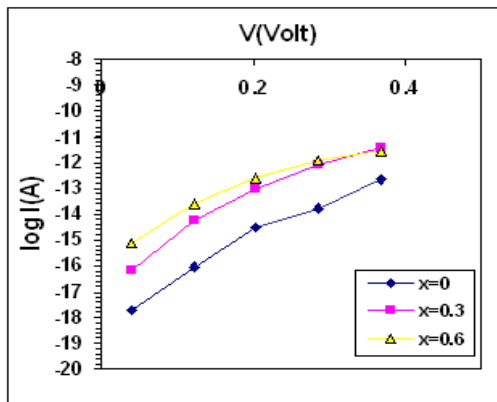


**Fig. 9:** I-V characteristics at forward bias voltage on semi-logarithm scale for  $\text{Cd}_2\text{Si}_{1-x}\text{Ge}_x\text{O}_4/\text{Si}$  diodes of different  $x$  values.

**Table 5:** The parameters which obtained from J-V characteristics for  $\text{Cd}_2\text{Si}_{1-x}\text{Ge}_x\text{O}_4/\text{Si}$  diodes with different  $x$  values.

x	$I_{S1} \times 10^{-9} (\text{A})$	$I_{S2} \times 10^{-3} (\text{A})$	$\beta$	$A (\text{V})^{-1}$	R.F
0	8.35	3.06	1.97	3.37	3.95
0.3	50.56	20.50	2.01	3.95	11.26
0.6	151.9	83.15	2.50	5.96	12.80

The  $\text{Cd}_2\text{Si}_{1-x}\text{Ge}_x\text{O}_4/\text{Si}$  diodes photocurrent density as a function of voltage under steady state illumination intensity ( $32 \text{ mW/cm}^2$ ) are presented in Fig. 10.

It is clear from this figure that the photocurrent increase with increasing the bias voltage, specially in reverse bias in spite of the depletion region width increase the photocurrent continuously increases.

This happen because increase the electric field sweeps the carriers out of the depletion region, with existing illumination, electron-hole pairs are created near the junction. If the e-h pairs is generated within a diffusion length ( $L_n, L_p$ ) of the transition region, the electrons can diffuse to the junction and swept down the barrier to the n side.

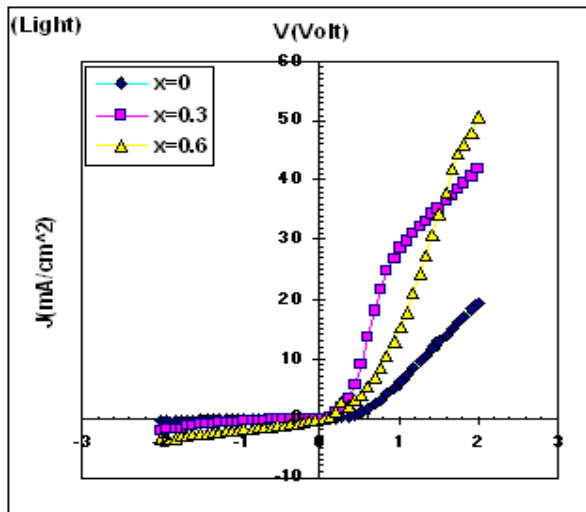


**Fig.10:** The relation between  $J_{ph}$  and bias voltage for  $\text{Cd}_2\text{Si}_{1-x}\text{Ge}_x\text{O}_4/\text{Si}$  diodes of different  $x$  values.

The resulting current is called the generation current since its magnitude depends entirely on the rate of generation of e-h pairs. So that the photocurrent is function of generation and diffusion mechanism as in the following equation (Grove, A.S., 1976).

$$I_{ph} = q a G_{ph} (L_p + L_n + W) \quad (4)$$

where  $G_{ph}$  generation rate of photocarriers,  $L_p$  and  $L_n$  are the diffusion length of holes and electrons, respectively.

#### c- Gas Sensor:

Semiconducting metal oxide gas sensors are commonly used for environmental monitoring and industrial applications due to their advantages such as small dimensions, low cost and convenient operation (Gupta, S. K., 2010). Also these materials have physical and chemical stability (Shishyanu, S. T., 2005).

The  $\text{Cd}_2\text{Si}_{1-x}\text{Ge}_x\text{O}_4$  sensor elements gas sensitivity and response-recovery characteristics

have been evaluated at room temperature for 160 ppm NO<sub>2</sub> gas.

A typical gas sensing measurement consisted sensors exposure to the toxic gas ( $\text{NO}_2$ ) and recorded the change in the films resistance.

The resistance response of each sensor structure was transformed into a sensitivity value which is one of the important parameters of gas sensors, the sensitivity of the metal oxide based materials, will change with the factors influencing the surface reactions, such as chemical components, surface modification and microstructures of sensing layers, temperature and humidity (Wang, C.,2010).

The sensitivity ( $S$ ) for oxidizing gases commonly defend as

where  $R_g$  is the sensor resistance influenced by the  $\text{NO}_2$  gas,  $R_0$  the sensor resistance in the air.

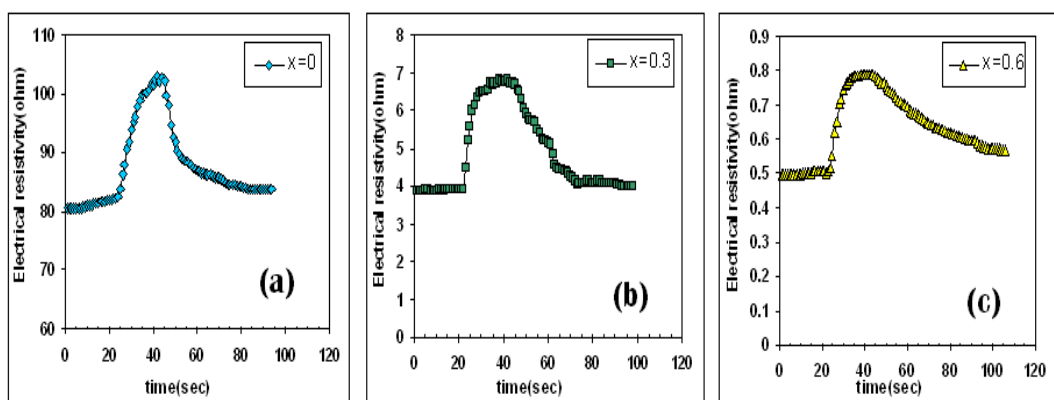


**Fig. 11:** Dynamic response of  $\text{Cd}_2\text{Si}_{1-x}\text{Ge}_x\text{O}_4$  gas sensors to  $\text{NO}_2$  gas at different x values.

When oxidizing gas molecules such as nitrogen dioxide come into contact with film surface, they may interact with this oxygen and this reaction consumed the conduction electrons and subsequent detection reaction lead to increase the barrier height and decrease the surface conductance(- Moseley, P.T., 1992).

The response of the films to  $\text{NO}_2$  gas can be explained by the equation

**Table 6:** Gas sensor measurement data of  $\text{Cd}_2\text{Si}_{1-x}\text{Ge}_x\text{O}_4$  sensors at different x values.

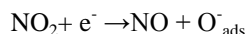
Table 6. Gas sensor measurement data of $\text{Cd}_2\text{Sn}_{1-x}\text{Ge}_x\text{O}_4$ sensors at different x values.			
x	Rise time (Sec)	Recovery time (Sec)	Sensitivity
0	17	27	0.25
0.3	15	29	0.73
0.6	17	51	0.55

### ***Conclusions:***

The effect of Ge concentration on the optical and electrical properties of amorphous  $\text{Cd}_2\text{Si}_{1-x}\text{Ge}_x\text{O}_4$  thin films deposited by pulsed-Laser deposition technique were studied. All films have a medium transmittance in the visible and NIR region. The films show a direct transition with a blue shift of the fundamental optical absorption edge when Ge ratio

Fig. 11 shows the dynamic response of  $\text{Cd}_2\text{Si}_{1-x}\text{Ge}_x\text{O}_4$  sensor to 160 ppm  $\text{NO}_2$  at room temperature. The characteristic behavior of the resistance increase of the sensors upon detecting  $\text{NO}_2$  gas is typical for n-type semiconductor oxide gas sensors. When the  $\text{NO}_2$  gas was introduced into the test chamber, the resistance of the sensor increased and soon afterwards it became saturated. When the gas was turned-off, the resistance of the sensor was decreased.

The surface layer of the  $\text{Cd}_2\text{Si}_{1-x}\text{Ge}_x\text{O}_4$  based gas sensors is responsible for the sensing properties. The mechanisms normally accepted for semiconductor sensors assume that the oxygen adsorbed on the film surface at room temperature. These reactions in the oxides surface layer change the concentration of the conduction electrons providing the sensing property.



In these reactions the electrons are extracted from the conduction band thus the resistivity of  $\text{Cd}_2\text{Si}_{1-x}\text{Ge}_x\text{O}_4$  increases (Shishiyano, S. T., 2005).

The  $\text{Cd}_2\text{Si}_{1-x}\text{Ge}_x\text{O}_4$  sensors element have relatively fast response time and the  $\text{Cd}_2\text{Si}_{0.7}\text{Ge}_{0.3}\text{O}_4$  sensor has higher sensitivity compared to the other composition ( $\text{Cd}_2\text{SiO}_4$ , and  $\text{Cd}_2\text{Si}_{0.4}\text{Ge}_{0.6}\text{O}_4$ ) as shown in Table 6.

increases. Hall measurements revealed n-type electrical conduction with a high mobility. The electrical properties measurements of  $\text{Cd}_2\text{Si}_{1-x}\text{Ge}_x\text{O}_4$ /Si diodes showed that the impurity profile near the junction is abrupt and the width of depletion layer decrease with increasing Ge ratio. The mechanism of the current transport in the forward condition coincides with recombination-tunneling model.

These diodes have a good rectification properties, and the rectification coefficient increases with increasing Ge ratio in this compound.  $\text{Cd}_2\text{Si}_{1-x}\text{Ge}_x\text{O}_4$  films have a good sensing to  $\text{NO}_2$  gas at room temperature , and the higher sensitivity recorded was 73% for  $\text{Cd}_2\text{Si}_{0.7}\text{Ge}_{0.3}\text{O}_4$  films.

## REFERENCES

- Alnaimi, S.M. and M.N. AL-Dileamy, 2007. Determination of the Optical Constants of Cadmium Stannate ( $\text{Cd}_2\text{SnO}_4$ ) Films. International Journal of Pure and Applied Physics, 3(1): 30-39.
- Barquinha, P., R. Martins, L. Pereira and E. Fortunato, 2012. Transparent Oxide Electronics From Materials to Devices, first published , John Wiley & Sons, Ltd publication, United Kingdom.
- Kumaravel, R., V. Krishnakumar, V. Gokulakrishnan, K. Ramamurthi, K. Jeganathan, 2010. Effect of annealing on the electrical. Optical and structural properties of cadmium stannate thin films prepared by spray pyrolysis technique, Thin Solid Films, 518: 2271-2274.
- Abd El-Raheem, M., M.S. Rasheed, H.E. Ahmed, M.S. Abd El-Aal, H.H. Al-Ofi, E.E. Mohamed, 2012. Characterization of Thin Films of Cd - doped SnO for Optoelectronic Applications. Advances in Applied Science Research, 3(1): 227-234.
- Masanori, K., D.I. Mendeleevs, 2002. Concepts of Chemical Elements and the Principles of Chemistry. Bulletin for the History of Chemistry, 27: 4-16.
- Washio, K., 2003. SiGe HBT and BiCMOS technologies for optical transmission and wireless communication systems. IEEE Transactions on Electron Devices, 50: 656.
- Hidalgo, P., E. Liberti, Y. Lazcano, B. Me'ndez and J. Piqueras, 2009.  $\text{GeO}_2$  Nanowires Doped with Optically Active Ions. J. Phys. Chem., C 113: 17200-17205.
- Hidalgo, P., B. Mendez and J. Piqueras, 2007. High aspect ratio  $\text{GeO}_2$  nano- and microwires with waveguiding behaviour. Nanotechnology, 18: 1-4.
- Geological, S., 2008. Germanium – Statistics and Information, U.S. Geological Survey, Mineral Commodity Summaries.
- Teal, H., K. Gordon, 1976. Single Crystals of Germanium and Silicon-Basic to the Transistor and Integrated Circuit. IEEE Transactions on Electron Devices, 7: 621-639.
- Narushima, S., H. Hosono, J. Jisun, T. Yoko, K. Shimakawa, 2000. Electronic transport and optical properties of proton-implanted amorphous  $2\text{CdO} - \text{GeO}_2$  films. Journal of Non-Crystalline Solids, 274: 313-318.
- Ikhmayies, S., R.Ahmad, 2010, A comparison between the electrical and optical properties of  $\text{CdS}:In$  thin films for two doping ratios. Jordan Journal of Mechanical and Industrial Engineering, 4(1): 111-116.
- Salman, Gh., E. Kareem, A.N. Naje, 2014. Optical and electrical properties of CU doped CdO thin films for detector applications. International Journal of Innovative Science, Engineering & Technology, 1: 147-151.
- Amaechi, C.I., S.C. Ezugwu, F.I. Ezema, P.U. Asogwa, A.E. Ajuba, 2011. Composition, Optical And Solid State Properties OF Quaternary  $\text{Cd}_{0.39}\text{Ba}_{0.28}\text{S}_{0.10}\text{O}_{0.23}$  Films. J. of Non-Oxide Glasses, 3: 1-7.
- Milnes, A.G. and D.L. Feucht, 1972. Heterojunctions and Metal- Semiconductor Juncctions. Academic Press, New York and London.
- Sharma, B.L., and R.K. Purohil, 1974. Semiconductor Heterojunctions. First edition, Pergamon press, Oxford, New York.
- Sarusi, G., A. Zemel, Ariel Sher and D. Eger, 1994. Forward tunneling current in  $\text{HgCdTe}$  photodiodes. J. Appl. Phys., 76: 4420-4425.
- Wenus, J., J. Rutkowski and A. Rogalski, 2003. Analysis of VLWIR  $\text{HgCdTe}$  photodiode performance. Opto-Electronics Review, 11(2): 143-149.
- Kim, W., C. Won, 2002. Optoelectronic Properties of Spray Deposited  $\text{SnO}_2:\text{F}$  Thin Films For Window Materials in Solar Cells. Applied Physics Letters, 80: 4006-4010.
- Mousa, A.M., and A.J. Haider, 2011. Performance of a Nano  $\text{CdS}/\text{Si}$  Hetrojunction Deposited by CBD. Journal of Materials Science and Engineering A 1: 111-115.
- Ismail, R.A. and A.A. Hadi, 2003. Electrical characteristics of Si doped with Sb by laser annealing Electrical characteristics of Si doped with Sb by laser annealing. Turk J.Phys., 27: 145-152.
- Grove, A.S., 1976. Physics and Technology of Semiconductor Devices. John Wiley & sons, New York.
- Gupta, S.K., A. Joshi, and M. Kaur, 2010. Development of gas sensors using  $\text{ZnO}$  nanostructures. J. Chem. Sci., 122(1): 57-62.
- Shishiyano, S.T., T.S. Shishiyano and O.I. Lupon, 2005. Sensing characteristics of tin-doped  $\text{ZnO}$  thin films as  $\text{NO}_2$  gas sensor., Sensors and Actuators B., 107: 379-386.
- Wang, C., L. Yin, L. Zhang, D. Xiang and Rui Gao, 2010. Metal Oxide Gas Sensors: Sensitivity and Influencing Factors. Sensors, 10: 2088-2106.
- Moseley, P.T., 1992. Materials selection for semiconductor gas sensors. Sens.Actuators B., 6(1-3): 149-156.